

Simulation of Quantum-Ballistic Nanoswitches

A. Heigl and G. Wachutka

Institute for Physics of Electrotechnology, TU Munich, Arcisstraße 21, 80333 Munich, Germany
 e-mail: heigl@tep.ei.tum.de

INTRODUCTION

We study quantum-ballistic transport processes in nanoswitches realized by the use of modulation doped heterostructures such as GaAs/AlGaAs layers. These structures have been modelled on the basis of a direct Schrödinger-Poisson approach taking into account also their non-linear behavior.

MODELLING

The electric current through a two-port structure is represented as quantum-ballistic current density

$$J = 2 \sum_{t \in T} \int j_{\varepsilon,t}(r) (f(\varepsilon, \mu_1) - f(\varepsilon, \mu_2)) d\varepsilon \quad (1)$$

This formula is actually the non-linear version of the well-known Landauer-Büttiker formula. Here, it is assumed that the ports are connected - via ideal electron waveguides - with charge reservoirs which are kept in thermodynamic equilibrium. This means that $f(\varepsilon, \mu)$ can be modelled as Fermi-Dirac distribution with μ as the electrochemical potential of the respective contact (Fig. 1).

The wavefunctions in the active area of the device are determined as solutions of the Schrödinger equation in effective-mass formulation

$$\left[-\frac{\hbar^2}{2} \nabla \frac{1}{m^*} \nabla + V_h - e\varphi + V_{xc}[n] - \varepsilon \right] \psi_{j,\varepsilon} = 0 \quad (2)$$

with the electrostatic potential φ , the exchange-correlation potential V_{xc} and the step potential of the heterostructure V_h . At the contacts, scattering boundary conditions are assumed. This yields an energy-dependent transmission probability for the scattering states. The resulting wavefunctions are self-consistently coupled to the Poisson equation by the temperature-dependent electron density

$$\rho(r) = \int \sum_j g(\varepsilon) f_j(\varepsilon) |\psi_{j,\varepsilon}(r)|^2 d\varepsilon \quad (3)$$

The electrostatic potential is calculated using the Green's function method. Practically this approach

is equivalent to adding the convolution $G \star \rho$ to the electronic potential without the electrostatic Coulomb potential according to

$$V(r) = V_h(r) + V_{xc}[n](r) - eG(r) \star \rho(r) \quad (4)$$

The assumption that the top surface is metallized leads to the following Green's function:

$$G(r) = \frac{1}{4\pi\varepsilon} \left(\frac{1}{|r|} - \frac{1}{|r-d|} \right) \quad (5)$$

Another modification of the electronic potential originates from the gate-voltages. These will change the number of occupied states of the 2D electron gas at the heterojunction.

RESULTS

The simulations were performed using the 3D simulator SIMNAD [1] and a new non-linear version of the simulator HIGHBIAS [2]. As a first test problem we considered a quantum-wire fabricated and characterized at the University of Würzburg [3]. This structure is built from 40 nm deep and 80 nm wide trenches forming a 100 nm quantum-wire. At a depth of 40 nm underneath the surface a 2D electron gas is easily recognized (Figs. 2, 3).

The influence of the gate voltage is demonstrated by the output characteristics displayed in Fig. 5. We obtain a fairly good agreement between simulation and measurement (Fig. 6) proving the quality of our approach.

ACKNOWLEDGMENT

This project is funded by the Bavarian Science Foundation within the research consortium for nanoelectronics FORNEL.

REFERENCES

- [1] F.O. Heinz, *Simulation approaches for nanoscale semiconductor devices*, Dissertation, ETH Zürich (2004).
- [2] E. Forsberg and J.O.J. Weström, *Self-consistent simulations of mesoscopic devices operating under a finite bias*, Sol. State Electronics **48**, 1147 (2004).
- [3] L. Worschech and D. Hartmann, *Private communication*.

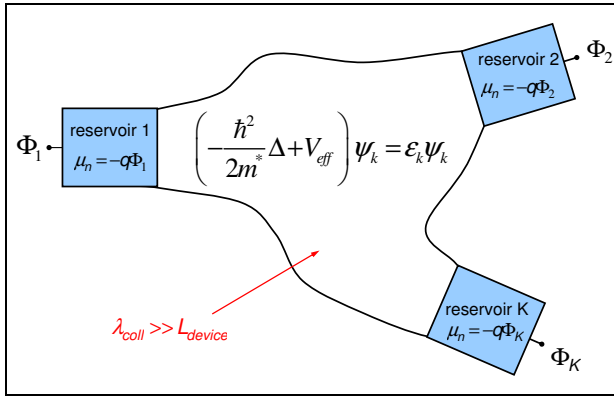


Fig. 1. Basic scheme of simulation domain and boundary conditions (within the active region of the device there are no inelastic scattering processes; only potential-scattering at V_{eff})

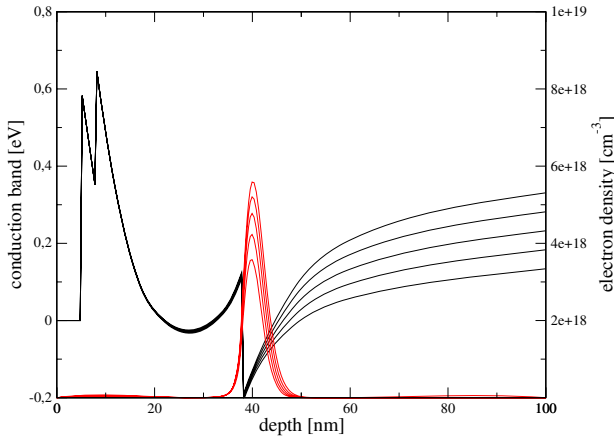


Fig. 2. Conduction band energy and electron density along a vertical cut at different gate voltages (see cut-line in Fig.4)

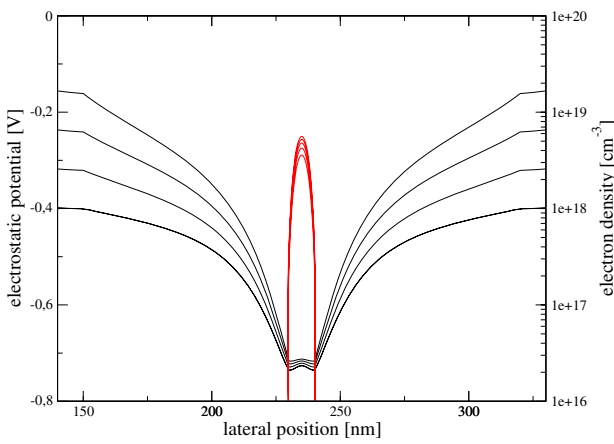


Fig. 3. Electron density and electrostatic potential along a lateral cut at different gate voltages (see cut-line in Fig.4)

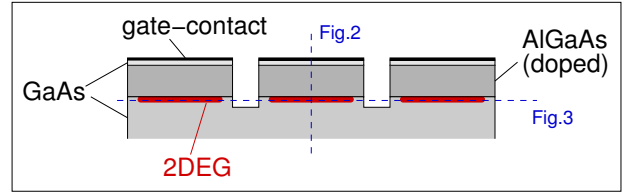


Fig. 4. Schematic view of the trench-controlled 2D quantum-wire structure (lateral cross section)

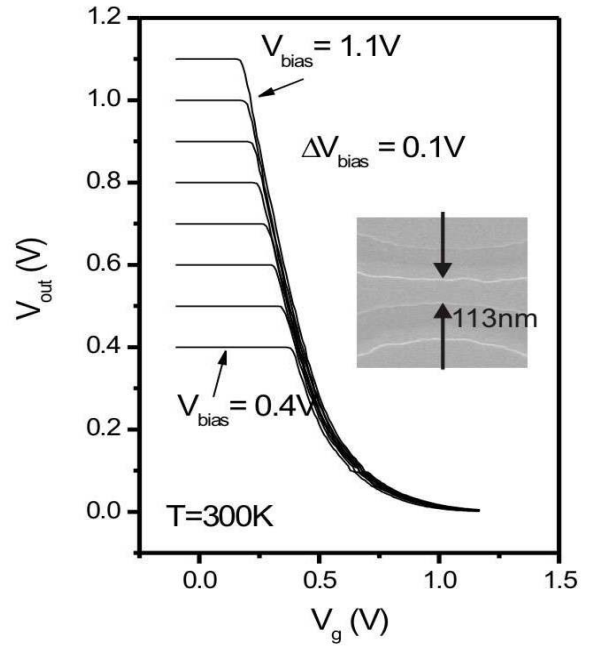


Fig. 5. Measured output characteristics of a quantum-wire structure (obtained from the University of Würzburg) [3]

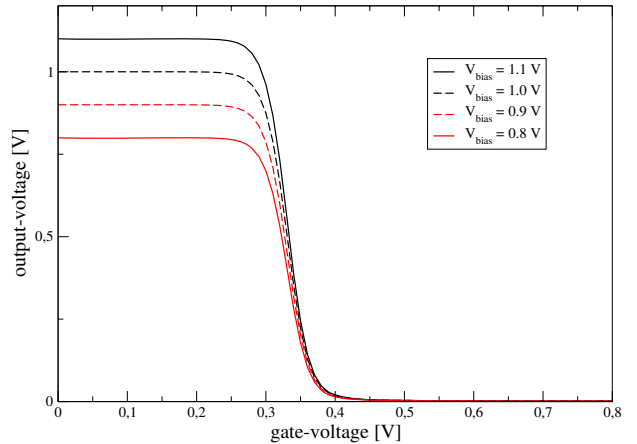


Fig. 6. Simulated output characteristics of a quantum-wire as calculated by SIMNAD